

Cryogenically probing the surface trap states of single nanowires passivated by self-assembled molecular monolayers

(Supporting Information)

Xingyan Zhao, Peng Tu, Jiajing He, Hong Zhu and Yaping Dan*

University of Michigan – Shanghai Jiao Tong University Joint Institute, Shanghai Jiao
Tong University, Shanghai 200240, China

*To whom correspondence should be addressed: yaping.dan@sjtu.edu.cn

S1. Lumerical FDTD and DEVICE Simulation Details

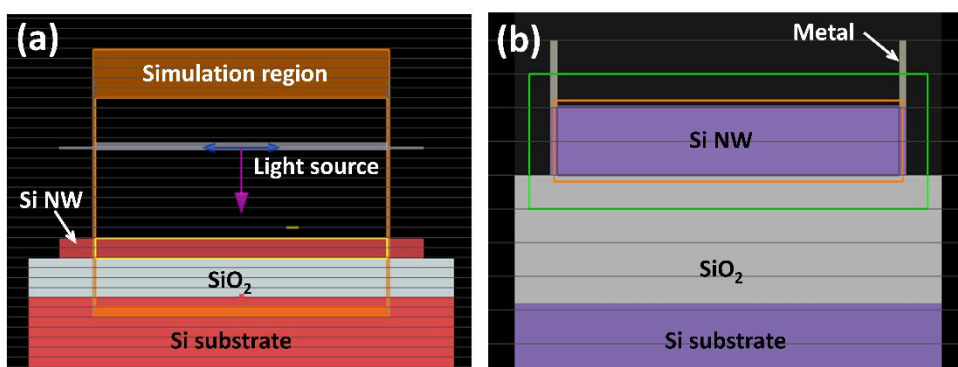


Fig.S1. (a) Optical simulation setup. (b). Electrical simulation setup. The green rectangle indicates the doping region. The orange region is the simulation region.

We used Lumerical FDTD software to calculate the generation rate for the photoconductance simulation. A planwave source with wavelength of 405nm was used in the optical simulation. The light intensity was set to 6.6w/cm². The calculated generation rate inside the Si NW was then imported into the DEVICE module. Trap-assisted recombination, radiative recombination, surface recombination and auger recombination were included in the simulation. The mobility of the hole was obtained from Hall measurements shown in Fig.2 in the article. The mobility of

minority electrons is 3 times the hole mobility. The surface recombination velocity of Si/SiO₂ interface was adjusted to ensure that the simulated photoconductance is the same with the measured result in the experiment.

S2. N_{it} and D_{it} Calculation

The N_{it} and D_{it} are calculated as follows:

The number of excess holes that contribute to the trap induced photoconductance:

$$\Delta p_2 = \frac{\sigma_T L}{q u_p A_c}$$

where L is the nanowire length, A_c is the nanowire cross section

Surface concentration of trapped electrons:

$$n_{it} = \frac{\Delta p_2 \cdot V_{NW}}{A}$$

where V_{NW} is the nanowire volume, A is the nanowire surface area

The surface trap states density:

$$D_{it} = \frac{\Delta n_{it}}{\Delta(E_F^n - E_i)}$$

S3. Computational Method

The density functional theory (DFT) calculations with the Perdew-Burke-Ernzerhof (PBE)¹ generalized gradient approximation (GGA) and projector augmented wave (PAW)² pseudopotentials were performed within the Vienna Ab Initio Simulation Package (VASP)³. The energy cut-off for the plane wave expansions of 520 eV and a 4*4*1 k-points mesh were used for 1*1 surface unit cell calculations of silicon slabs.

Three kinds of silicon slabs were considered in this work. The first one was constructed by superposing the β-cristobalite SiO₂ structure onto 1*1 (001) surface of the diamond Si structure. The Si(001)/SiO₂ interfaces⁴⁻⁸ have been studied previously using DFT calculations. Similar to the models in Seino's work⁸, we considered three Si(001)/SiO₂ interface models, (i) the bridge-oxygen model (BOM) with a substitutional O atom in the topmost Si layer, (ii) the double-bond model (DBM) with

Si dangling-bond saturation by addition of a single double-bonded oxygen atom (Si=O), and (iii) the hydrogen model (HGM) where a Si dangling bond at the interface is saturated by a hydrogen atom (Si-H). By using HGM as reference, for example, BOM can be obtained by adding one oxygen atom and subtracting two hydrogen atoms in the basis of HGM. The formation energy of BOM interface with respect to HGM interface is -2.39 eV according to the above reaction. The formation energy of DBM interface obtained in the same way is -0.88eV. Therefore, we were specifically interested in the density of states (DoS) of the BOM type Si/SiO₂ slab, whose structure is shown in Fig.S2a. The second slab model was constructed by passivating 1*1 Si(001) surface with hexadecane molecular ((CH₂)₁₅CH₃). Here we used a shorter carbon chain (CH₂)₅CH₃ (shown in Fig.S2b) which captured the interface bonding but converged faster. One dangling bond of interface Si bonds to C and the other bonds to oxygen. The third slab was composed of Si(001) and Diethyl 1-propylphosphonate (DPP), as Fig.S2c shows. The top surface of silicon slab is either bonded to DPP or passivated by hydrogen atoms. Due to the lateral size of DPP, we used 2*3 surface cell of Si(001). In all models, the dangling bonds of the bottom Si surface in the last layer were passivated by hydrogen atoms.

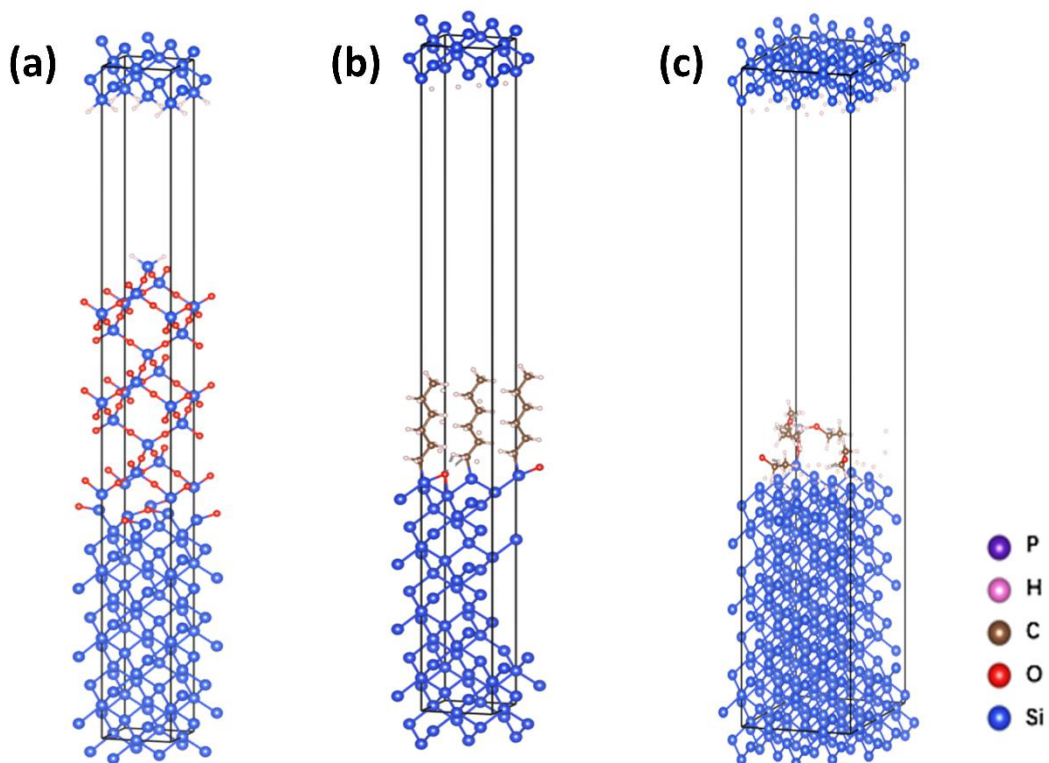


Fig. S2. The structure of (a) Si/SiO₂ BOM, (b) Si/Hexadecane, (c) Si/DPP slabs

The E_c , E_v and E_i (the average of E_v and E_c) for the bulk-like region Si were calculated and shown in Table S1. Then the DoS of these three slabs are aligned based on E_i . Finally, the aligned total DoS of three systems, namely Si/SiO₂ BOM, Si/Hexadecane, and Si/DPP were plotted in Fig. S3.

Table S1. The energy of VBM (E_v), CBM (E_c) and middle bandgap energy level ($E_i = 1/2(E_v + E_c)$) of the bulk-like region Si in (a) Si/SiO₂ BOM, (b) Si/Hexadecane, (c) Si/DPP slabs, where the unit is eV.

| | E_v | E_c | E_i |
|---------------|--------|-------|-------|
| Si/Dry oxide | 1.733 | 2.149 | 1.941 |
| Si/Hexadecane | 0.821 | 1.304 | 1.063 |
| Si/DPP | -0.116 | 0.429 | 0.157 |

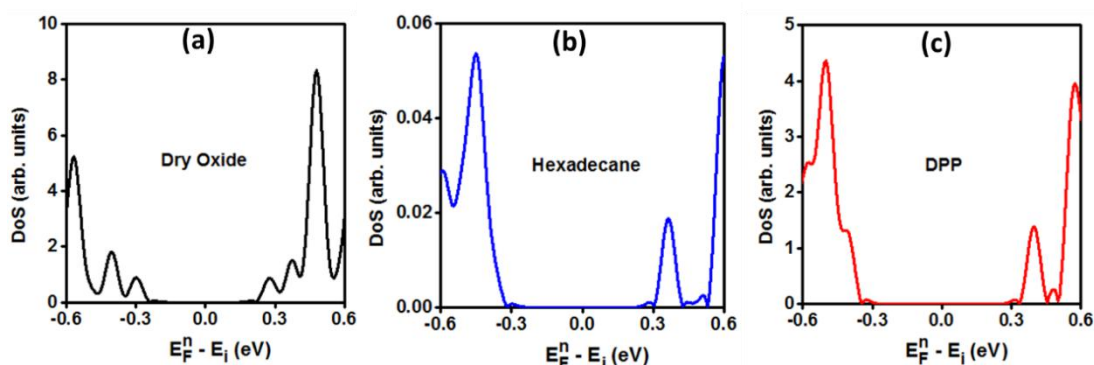


Fig. S3. Density of States in the full bandgap region. (a) Si/Dry oxide (b) Si/Hexadecane (c) Si/DPP

S4. XPS Data Analysis

We employed the XPS method to verify whether the hexadecane and the DPP molecules were bounded to the silicon surfaces. The XPS data of the blank sample, hexadecane and DPP passivated silicon wafer are shown in Fig. S4. The graft of the molecules was verified by comparing the XPS data of the element Si (2p and 2s, 99.9 and 151.1 eV, respectively), C (1s, 285.4 eV), and O (1s, 532.7 eV) with and without self-assembled monolayer passivation. For hexadecane, we can find the

carbon ratio increased a lot due to the fact that the hexadecane molecular is rich of carbon. The C=C bond makes the self-assembled molecular (SAM) monolayer process more efficient. The chain structure can help the passivation process due to its small footprints. DPP molecules were immobilized onto the silicon wafer by forming Si-O-P covalent bonds. Fewer dangling bonds will be passivated by the DPP molecules due to the larger footprint of the molecules. In the XPS data, we can find that the carbon ratio is much smaller than the hexadecane but larger than blank sample. The decrease of O ratio can also indicate the successful SAM passivation.

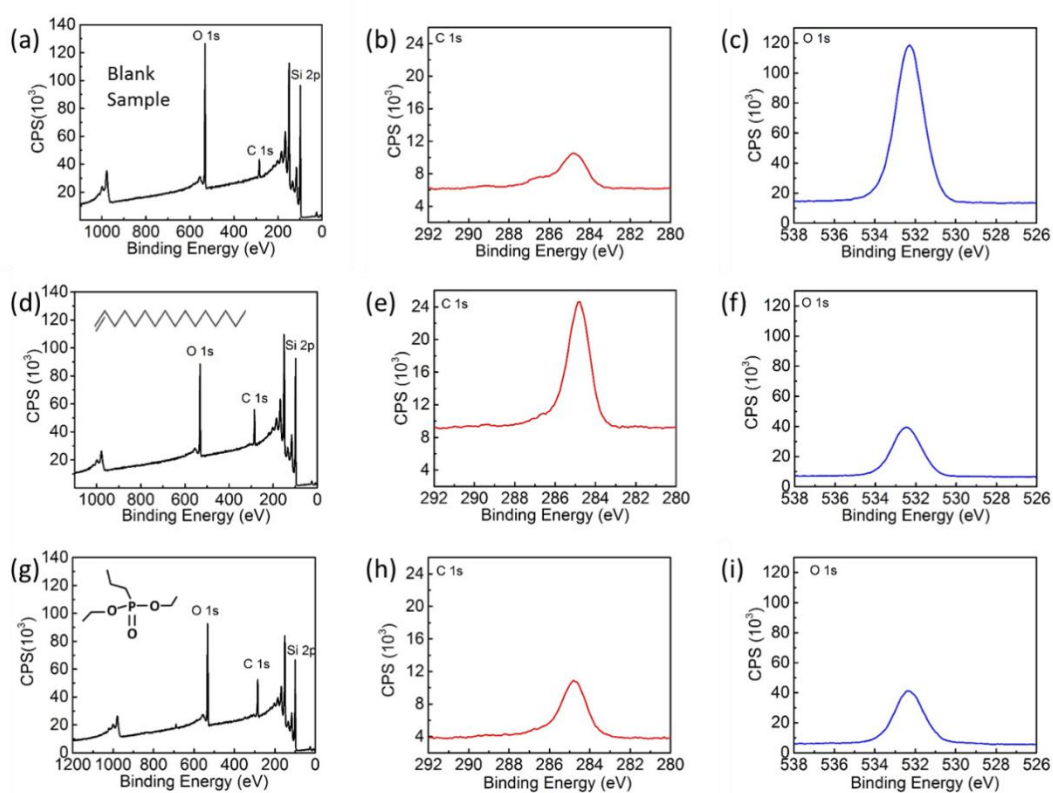


Fig.S4. XPS data of the silicon wafers before and after the self-assembled monolayer passivation process. (a,b,c) XPS survey spectra and narrow scan of the C 1s and O 1s region of blank sample, treated with HF solution and then immersed in mesitylene. (d,e,f) XPS survey spectra and narrow scan of the C 1s and O 1s region of the sample passivated by hexadecane (structure inset in figure d). (g,h,i) XPS survey spectra and narrow scan of the C 1s and O 1s region of the sample passivated by DPP (structure inset in figure g)

S5. As fabricated SiNW device

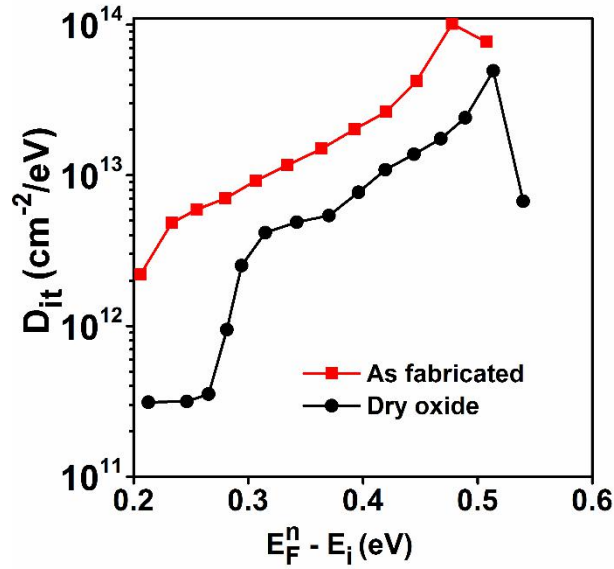


Fig.S5. Experimental data of surface trap states density distribution of our as fabricated and dry SiO₂ passivated nanowire devices.

S6. Transient photocurrent response

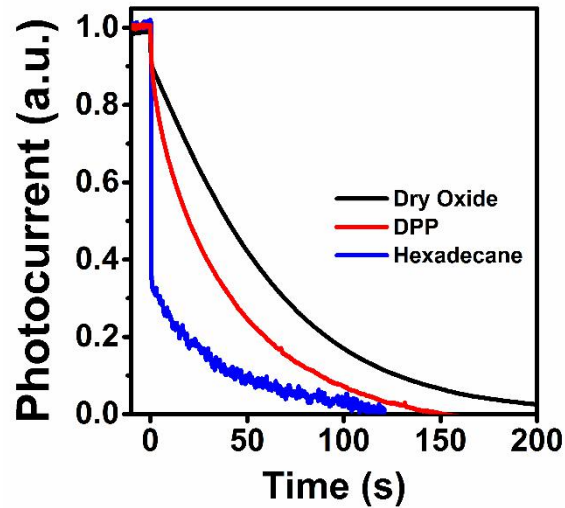


Fig.S6. Transient photocurrent response of the nanowire devices with different surface passivation. $E_F^n - E_i \sim 0.40\text{eV}$

When the quasi fermi energy level E_F^n is around 0.40eV about E_i , trap states density of the SiO₂ passivated nanowire device is much higher than the Hexadecane and DPP passivated device (Fig.4a in the manuscript). Thus the SiO₂ passivated device has a longer trap lifetime than Hexadecane and DPP passivated device. And the Hexadecane passivated device has a shortest trap lifetime due to its lowest trap states density.

Reference

- ¹J. P. Perdew, K. Burke, and M. Ernzerhof, *Physical Review Letters* **77** (18), 3865 (1996).
- ²P. E. Blöchl, O. Jepsen, and O. K. Andersen, *Physical Review B* **49** (23), 16223 (1994).
- ³G. Kresse, and J. Furthmüller, *Physical Review B* **54** (16), 11169 (1996).
- ⁴P. Carrier, L. J. Lewis, and M. W. C. Dharma-wardana, *Physical Review B* **64** (19), 195330 (2001).
- ⁵T. Yamasaki, C. Kaneta, T. Uchiyama, T. Uda, and K. Terakura, *Physical Review B* **63** (11), 115314 (2001).
- ⁶G. Feliciano, B. Angelo, and P. Alfredo, *Journal of Physics: Condensed Matter* **17** (21), S2065 (2005).
- ⁷K. Seino, J.-M. Wagner, and F. Bechstedt, *Applied Physics Letters* **90** (25), 253109 (2007).
- ⁸K. Seino, and F. Bechstedt, *Semiconductor Science and Technology* **26** (1), 014024 (2011).